



Spatiotemporal Clustering of Repeated Super-Resolution Localizations via Linear Assignment Problem

David J. Schodt and Keith A. Lidke*

Department of Physics and Astronomy, University of New Mexico, Albuquerque, NM, United States

OPEN ACCESS

Edited by:

Christian Franke,
Friedrich Schiller University Jena,
Germany

Reviewed by:

Perrine Paul-Gilloteaux,
INSERM US16 Santé François
Bonamy, France
Jean-Karim Hériché,
European Molecular Biology
Laboratory Heidelberg, Germany
Alexander Raymond Small,
California State Polytechnic University,
United States

*Correspondence:

Keith A. Lidke
klidke@unm.edu

Specialty section:

This article was submitted to
Computational Biolmaging,
a section of the journal
Frontiers in Bioinformatics

Received: 12 June 2021

Accepted: 04 October 2021

Published: 20 October 2021

Citation:

Schodt DJ and Lidke KA (2021)
Spatiotemporal Clustering of Repeated
Super-Resolution Localizations via
Linear Assignment Problem.
Front. Bioinform. 1:724325.
doi: 10.3389/fbinf.2021.724325

Many fluorescence super-resolution techniques, such as (d)STORM, PALM, and DNA-PAINT, generate datasets wherein multiple localizations across many camera frames may arise from a single blinking event of an emitter. These repeated localizations not only hinder interpretation and analysis of such datasets, but also represent an incomplete use of the fluorescence photons. Such localizations are typically combined into a single localization either by clustering with hard distance and time thresholds, or by classical hypothesis testing assuming Gaussian localization errors. In this work, we describe a method for clustering that accounts for localization precision, local emitter density estimates, and a kinetic model for blinking which is used to optimize connections within a group of spatiotemporally colocated localizations.

Keywords: fluorescence microscopy, super-resolution, image analysis, computational modeling, single molecule techniques

1 INTRODUCTION

Fluorescence super-resolution methods have grown to be vital imaging techniques in many research areas, particularly in the biological sciences. Single Molecule Localization Microscopy (SMLM) methods take advantage of an extreme form of temporal independence where individual sources blink on and off with little spatial-temporal overlap from other “on” sources. Many of these techniques, such as (d)STORM (Rust et al., 2006; Heilemann et al., 2008), PALM (Betzig et al., 2006; Hess et al., 2006), and DNA-PAINT (Jungmann et al., 2010), are relatively easy to implement on common fluorescence microscopes with little to no modifications. By finding the center of distinct PSFs arising from independent “on” sources as observed on a camera, SMLM data is reduced to a set of PSF center coordinates, or localizations, and their associated precisions. The subsequent processing of these localizations can have significant impacts on the final interpretation of the data.

Despite extensive research into optimally localizing emitters (Small and Stahlheber, 2014; Deschout et al., 2014; Sage et al., 2019), little effort has been spent on what we will henceforth refer to as the frame-connection problem. SMLM methods produce data with multiple localizations in subsequent/near-subsequent frames which are likely the result of a single blinking event of a single emitter. Specifically, a single visible emitter may appear in multiple frames, with each frame potentially producing a new localization of that emitter. The frame-connection problem deals with combining these repeated localizations into a single localization with higher precision. To the best of our knowledge, only two solutions to the frame-connection problem are in use: 1) combining any localizations within N frames and d pixels of one another, as is done in the popular ThunderSTORM package (Ovesný et al., 2014) (we'll refer to this method as the “classical” approach); or 2) by a hypothesis test assuming Gaussian

localization noise (“hypothesis test”) (Wester et al., 2021). A modification to the classical approach involves setting the separation threshold d to be some multiple of the localization error, as is done in the PYMEVisualize package (Marin et al., 2021) (referred to as “chaining” in that work and as “revised classical” here). The classical approach has the benefit of simplicity: its implementation is straightforward and accessible. The hypothesis testing approach makes use of localization error to test the null hypothesis that localizations came from the same emitter, however it neglects a calculation and comparison to the low-probability alternative hypothesis that a new emitter could have appeared in the same location. Both of these methods implicitly make use of the prior knowledge that multiple blinking events within a small spatiotemporal volume is rare in SMLM data.

To ensure information about the underlying structure of emitters is retained, an optimal frame-connection solution should exhibit minimal over-clustering. In other words, a frame-connection algorithm prone to connecting localizations from distinct emitters may reduce the quality of SMLM data. However, if a frame-connection algorithm is prone to under-clustering localizations from a single blinking event, its addition to the analysis pipeline may not represent much value. In that view, an optimal frame-connection solution must be capable of clustering those localizations which are very likely to have arisen from a single blinking event of a single emitter, all the while remaining sufficiently conservative in its connection assignments to minimize over-clustering.

The analysis of SMLM localizations can be classified into two categories: pre- and post-processing. Broadly speaking, pre-processing is a clean-up stage during which raw localizations are filtered without destroying the information they carry. Frame-connection should be considered pre-processing in the sense that its goal is to combine repeated localizations without destroying the temporal information carried by emitter blinking. In contrast, post-processing methods aim to condense/summarize the information carried by the localizations into descriptors of the underlying structure or process being observed. More general post-processing clustering methods, such as DBSCAN (Daszykowski et al., 2001), Voronoi tessellation (Levet et al., 2015), and BaGoL (Fazel et al., 2019b), differ from pre-clustering frame-connection in that they are not restricted to grouping observations of a single blinking event. Rather, post-processing clustering methods attempt to associate or make inference from all localizations of a single emitter.

The analysis of single-particle tracking (SPT) data aims to achieve a similar goal to frame-connection: associating multiple localizations over time to a single emitter. The ideal solution to the SPT problem is global across all connection possibilities; however, such a solution is not computationally feasible for realistic experiments. A locally greedy solution is prone to incorrect/missed connections, a problem exacerbated by emitter blinking and detection failure. As a result, many SPT analysis methods approximate a global solution by performing a locally greedy (in time) step to reduce the computational complexity. For example, the multiple target tracing (MTT) method (Sergé et al., 2008) considers only those connection hypotheses corresponding to a sliding spatiotemporal window. The method presented in

(Jaqaman et al., 2008) performs an initial frame-to-frame connection followed by a global gap closing procedure.

In this work, we present a novel solution to the single blinking event frame-connection problem which accounts for local emitter densities, fluorescent emission kinetics, and localizations missed in processing, which we refer to as linear assignment problem frame-connection (LAP-FC). Motivated by the success and robustness of the cost matrix method to solving the linear assignment problem (LAP) in SPT (Jaqaman et al., 2008), we formulate the frame-connection problem in terms of the costs of connecting/not connecting localizations. Our algorithm effectively groups all reasonable connection hypotheses in a pre-processing step (enabled by the typical brevity of blinking events in SMLM data), which allows us to find a globally optimal solution to the single blinking event frame-connection problem. We demonstrate that our algorithm outperforms the classical and hypothesis test methods in several situations typical of SMLM data with no to minimal evidence of over-clustering. Furthermore, our algorithm is in practice parameter-free, making it the ideal method for use by end users of SMLM data.

2 MATERIALS AND METHODS

Our solution to the frame-connection problem consists of three primary components: 1) pre-clustering of localizations into sets of connection candidates, 2) estimating local densities and kinetic rates from preclusters, and 3) making a maximum likelihood assignment of localizations to clusters, which is implemented as a LAP. In this section, we will describe our formulation of the frame-connection problem before describing the three components of our algorithm. A description of some commonly used variables used throughout this text is provided in **Table 1**.

2.1 Pre-Clustering

For a typical SMLM dataset, the number of localizations $n \sim 10^6$ makes finding a global solution to the LAP across all localizations computationally infeasible. As such, we perform a pre-clustering of localizations in a manner similar to the revised classical frame-connection solution as presented in (Marin et al., 2021). For a given localization, the spatial nearest neighbor within some frame gap and within some multiplier of its localization error (typically chosen to be five frames and 5, respectively) is found. If that nearest neighbor is already part of a cluster, the localization is incorporated into that same cluster. Otherwise, the localization and its nearest neighbor (if one exists) are defined as a new cluster. To ensure localizations aren't excluded from their ideal precluster, pre-clustering allows incorporation of multiple localizations within the same frame to the same cluster.

2.2 Estimating Local Emitter Densities and Kinetic Rates

To estimate local emitter densities and kinetic rates, we assume that each precluster will on average be representative of a single blinking event. That is, we assume that most preclusters consists

TABLE 1 | Description of commonly used variables.

Variable	Description	Units
k_{on}	transition rate from the emitter dark state to the on (visible) state	frame ⁻¹
k_{off}	transition rate from the emitter on state to the reversible off state	frame ⁻¹
k_{bleach}	transition rate from the emitter on state to the irreversible bleached state	frame ⁻¹
p_{miss}	probability of failing to localize a visible emitter	
n	total number of (pre-frame connection) localizations in the data	
n_c	number of localizations in a given precluster	
N_{emitters}	underlying number of emitters in the data	
ρ_0	initial underlying density of emitters in the first frame of data	emitters/pixel ²
ρ	underlying density of non-bleached emitters	emitters/pixel ²
ρ_{on}	density of emitters in the “on” state	emitters/pixel ²
ρ_{off}	density of emitters in the “off” state	emitters/pixel ²
N	number of spatial dimensions	
\mathbf{x}	vector of Cartesian coordinates $[x_1, x_2, \dots, x_N]$	pixels
Δx_i	separation between two localizations along the i -th dimension	pixels
$\sigma_{x_i,1}^2$	variance of the first localization in the i -th dimension	pixels ²
$\sigma_{x_i,2}^2$	variance of the second localization in the i -th dimension	pixels ²
$\sigma_{x_i}^2$	sum of the variances $\sigma_{x_i,1}^2 + \sigma_{x_i,2}^2$	pixels ²
f	integer frame number	frames
f_{end}	frame number corresponding to the last frame of the data	frames
N_D	number of candidate frames that have elapsed by the appearance of a localization	frames
N_f	number of candidate frames remaining after the appearance of a localization	frames
τ	approximate duty cycle of an emitter	
F	CDF of the nearest-neighbor distribution of localizations within 5 frames of one another	
δ	deviation of a nearest-neighbor distribution CDF F from the ideal CDF F_{ideal}	

of localizations of a single emitter blinking once with a duration of multiple frames. The rate parameters k_{on} , k_{off} and k_{bleach} , and the probability of missing a localization p_{miss} are estimated from the pre-clustered data as follows. The sum of the off rate and the bleaching rate $k_{\text{off}} + k_{\text{bleach}}$ is estimated from the cluster durations N (in frames) as

$$k_{\text{off}} + \widehat{k_{\text{bleach}}} = -\log\left(1 - \frac{1}{N}\right) \quad (1)$$

where $\widehat{\quad}$ denotes the mean value. The expression given in **Eq. 1** is derived assuming that cluster durations are geometrically distributed with the probability of turning off given by $1 - \exp[-(k_{\text{off}} + k_{\text{bleach}})]$ (the probability of turning off within $\Delta t = 1$ frames). The probability of missing a localization p_{miss} is estimated from the ratio of the number of localizations in a cluster n_c to the cluster’s duration N as

$$\hat{p}_{\text{miss}} = 1 - \frac{n_c}{N}$$

The expected cumulative number of localizations observed by frame f is given by

$$\langle n_{\text{cumulative}} \rangle (f) \approx N_{\text{emitters}} (1 - p_{\text{miss}}) \tau \left\{ \frac{1 - \exp[-\lambda_1 (f - 1)]}{\lambda_1} - \frac{1 - \exp[-\lambda_2 (f - 1)]}{\lambda_2} \right\} \quad (2)$$

with

$$\lambda_1 = k_{\text{bleach}} \frac{k_{\text{on}}}{k_{\text{on}} + k_{\text{off}} + k_{\text{bleach}}} \equiv k_{\text{bleach}} \tau$$

$$\lambda_2 = k_{\text{on}} + k_{\text{off}} + k_{\text{bleach}} - \lambda_1$$

where N_{emitters} is the total number of emitters present at the beginning of the experiment. **Eq. 2** was derived from the results presented in (Nino and Milstein, 2021) by assuming $k_{\text{on}} \ll k_{\text{off}}$ with no restriction on k_{bleach} and by accounting for p_{miss} . Similarly, the cumulative number of preclusters observed over time is of the form

$$\langle n_{\text{clusters cumulative}} \rangle (f) \approx k_{\text{off}} \langle n_{\text{cumulative}} \rangle (f) \quad (3)$$

According to **Eqs. 2, 3**, the off rate k_{off} can be estimated as n_{clusters}/n where n_{clusters} is the total number of preclusters and n is the total number of localizations. The bleaching rate k_{bleach} is then found by subtracting the estimate for k_{off} from **Eq. 1**. The on rate k_{on} and the underlying number of emitters N_{emitters} are then estimated by fitting the cumulative number of localizations to the model given in **Eq. 2**. Additional details about the parameter estimation procedures can be found in **Supplementary Text 1**.

The local pre-cluster density corresponding to each pre-cluster is estimated by finding the k (chosen to be two in this study) nearest pre-clusters and then computing $\rho_c = (k + 1)/\pi r_k^2$ where r_k is the distance to the k th nearest pre-cluster. The underlying local emitter density present at the beginning of the experiment is then estimated for each pre-cluster as

$$\hat{\rho}_{0,\text{local}} = \rho_c \frac{1}{\hat{k}_{\text{off}} \hat{\tau}} \frac{1}{1 - \hat{p}_{\text{miss}}} \left\{ \frac{1 - \exp[-\hat{\lambda}_1 (f_{\text{end}} - 1)]}{\hat{\lambda}_1} - \frac{1 - \exp[-\hat{\lambda}_2 (f_{\text{end}} - 1)]}{\hat{\lambda}_2} \right\}^{-1}$$

where f_{end} is the last frame containing localizations in the experiment. The density of on emitters ρ_{on} and the density of off emitters ρ_{off} are then estimated as

$$\hat{\rho}_{\text{on}}(f) = \hat{\rho}_{0,\text{local}} \hat{\tau} \left\{ \exp[-\hat{\lambda}_1(f-1)] - \exp[-\hat{\lambda}_2(f-1)] \right\}$$

$$\hat{\rho}_{\text{off}}(f) = \hat{\rho}_{\text{on}}(f) \frac{\hat{k}_{\text{off}}}{\hat{k}_{\text{on}}}$$

2.3 Frame-Connection via Minimization of Costs

The frame-connection problem can be thought of as a spatiotemporal clustering problem in which only one localization is allowed admittance to each cluster in each frame. In terms of the LAP, frame-connection concerns assigning each observed localization to one and only one cluster, with each assignment having an associated cost. In particular, frame-connection consists of “connection” costs, “birth” costs, and “death” costs. The connection costs are the costs for assigning a localization to an existing cluster. The birth costs are the costs for birthing a new emitter with the candidate localization being its first observation. The death costs are the costs for prohibiting assignment of any future localizations to an existing localization cluster. The costs are arranged in a square matrix such that the LAP solution permits only one assignment per row and column. We define each of these costs by assuming a three-state kinetic model for emitter blinking. The transition rates are defined as k_{on} , the rate from the (reversible) off state to the visible on state; k_{off} , the rate from the on state to the off state; and k_{bleach} , the rate from the on state to the (irreversible) bleached state. We additionally assume a constant probability of missing a localization (i.e., failing to localize a visible emitter) which we designate p_{miss} . Furthermore, the costs account for the local density of emitters $\rho(\mathbf{x}, f)$ where $\mathbf{x} = [x, y]$ is the precluster location and f is the frame number. Our procedure for estimating k_{on} , k_{off} , k_{bleach} , p_{miss} , and $\rho(\mathbf{x}, f)$ directly from the data is described in **section 2.2**.

The connection, birth, and death costs are defined to be the negative logarithm of the probabilities associated with the prescribed actions. The cost c_c of connecting two localizations is defined as follows:

$$c_c = -\log \left\{ \prod_{i=1}^N p(\Delta x_i | \sigma_{x_i}^2) \cdot p(\text{observe after missing localizations} | p_{\text{miss}}, \Delta f) \cdot p(\text{not turning off} | \Delta f) \right\}$$

where N is the number of dimensions (taken to be 2 for the present study), Δx_i is the separation between the two localizations along the i -th dimension, $\sigma_{x_i}^2 \equiv \sigma_{x_{i,1}}^2 + \sigma_{x_{i,2}}^2$ is the sum of the localization variances $\sigma_{x_{i,1}}^2$ for localization 1 and $\sigma_{x_{i,2}}^2$ for localization 2 in the i -th dimension, and $\Delta f > 0$ is the temporal separation between the two localizations. The probability terms are given by

$$p(\Delta x_i | \sigma_{x_i}^2) = \frac{1}{\sqrt{2\pi\sigma_{x_i}^2}} \exp\left(-\frac{\Delta x_i^2}{2\sigma_{x_i}^2}\right)$$

$$p(\text{observe after missing localizations} | p_{\text{miss}}, \Delta f) = (1 - p_{\text{miss}}) p_{\text{miss}}^{\Delta f - 1}$$

$$p(\text{not turning off} | \Delta f) = \exp[-(k_{\text{off}} + k_{\text{bleach}})\Delta f]$$

where the rate parameters are given in units of frame⁻¹. The cost of introducing a new emitter in frame M after N_p candidate frames (“birth” cost) is given by

$$c_b = -\log \left\{ p(\text{new emitter turning on} | k_{\text{on}}, \rho_{\text{off}}(\mathbf{x}, f), N_p) \cdot p(\text{not missing localization} | p_{\text{miss}}) \right. \\ \left. + p(\text{observe after missing localizations} | p_{\text{miss}}, N_p, \rho_{\text{on}}(\mathbf{x}, f)) \right\}$$

$$= -\log \left\{ \rho_{\text{off}}(\mathbf{x}, M) [1 - \exp(-k_{\text{on}})] \exp(-k_{\text{on}} N_p) (1 - p_{\text{miss}}) \right. \\ \left. + \rho_{\text{on}}(\mathbf{x}, M - N_p) (1 - p_{\text{miss}}) p_{\text{miss}}^{N_p} \right\}$$

where $\rho_{\text{off}}(\mathbf{x}, f)$ is the local density of emitters in the off state, and $\rho_{\text{on}}(\mathbf{x}, f)$ is the local density of emitters in the on state (see **section 2.2**). The cost of not observing an emitter for the remaining N_f candidate frames (“death” cost) is given by

$$c_d = -\log \left\{ p(\text{bleaching} | k_{\text{bleach}}) + p(\text{turn off} | k_{\text{off}}) + p(\text{missing localizations} | p_{\text{miss}}, N_f) \right\}$$

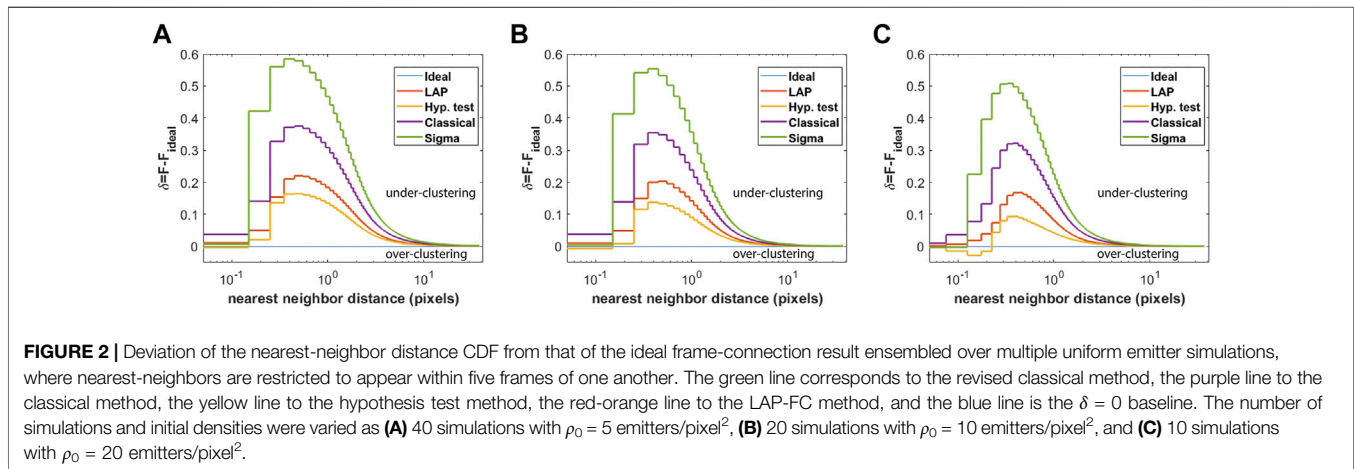
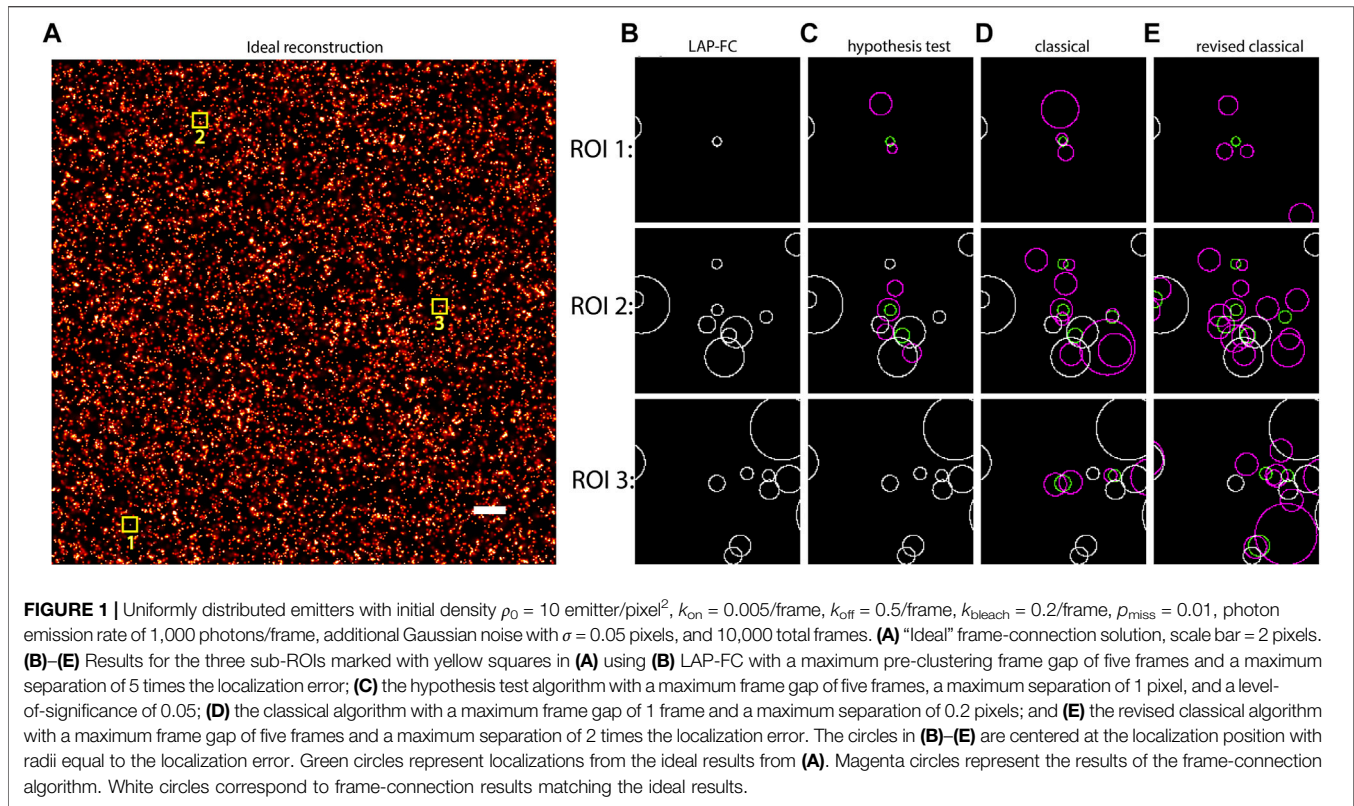
$$= -\log \left\{ [1 - \exp(-k_{\text{bleach}})] + [1 - \exp(-k_{\text{off}})] + p_{\text{miss}}^{N_f} \right\}$$

As in (Jaqaman et al., 2008), we arrange our LAP costs in a square block matrix composed of four equal sized square sub-matrices, with each sub-matrix being $n_c \times n_c$ for n_c localizations within a given precluster. The upper-left block matrix contains the connection costs between a localization identified by its row index with a localization identified by its column index, arranged as an upper-triangular matrix (to prohibit selection pairs of row m to column n and row n to column m) and divided by two to account for the definition of the bottom-right auxiliary block costs (see below). The bottom-left block contains the birth costs for the localizations identified by the column index. The upper-right block contains the death costs for the localizations identified by the row index. The bottom-right block, to which we attribute no physical significance, is defined to be the transpose of the upper-left connection block, as assignments in the upper-left block lead to the same assignments in the (transposed) lower-right block. All cost matrix entries containing a prohibited selection (e.g., main diagonal terms, which represent connection of a localization to itself) are set to a non-link marker, which tells the LAP solver not to select those entries. Costs that are infinite or otherwise invalid (i.e., not a number) are set to twice the sum of all valid costs to ensure they are only selected when no other assignment is available. The LAP is then solved using the Jonker-Volgenant algorithm (Jonker and Volgenant, 1987), which assigns each localization to a single cluster of localizations. This process is then repeated for each pre-cluster of localizations to yield the final frame-connected set of localizations.

Localizations connected by the frame-connection algorithm are combined assuming they each represent independent samples from a Gaussian distribution. The resulting position of the m frame-connected localizations is taken to be the maximum-likelihood estimate for the position \mathbf{x}

$$\hat{\mathbf{x}} = \frac{\sum_{i=1}^m \mathbf{x}_i / \sigma_i^2}{\sum_{i=1}^m 1 / \sigma_i^2} \quad (4)$$

and the localization error for the frame-connected localization is taken to be the inverse of the Fisher information

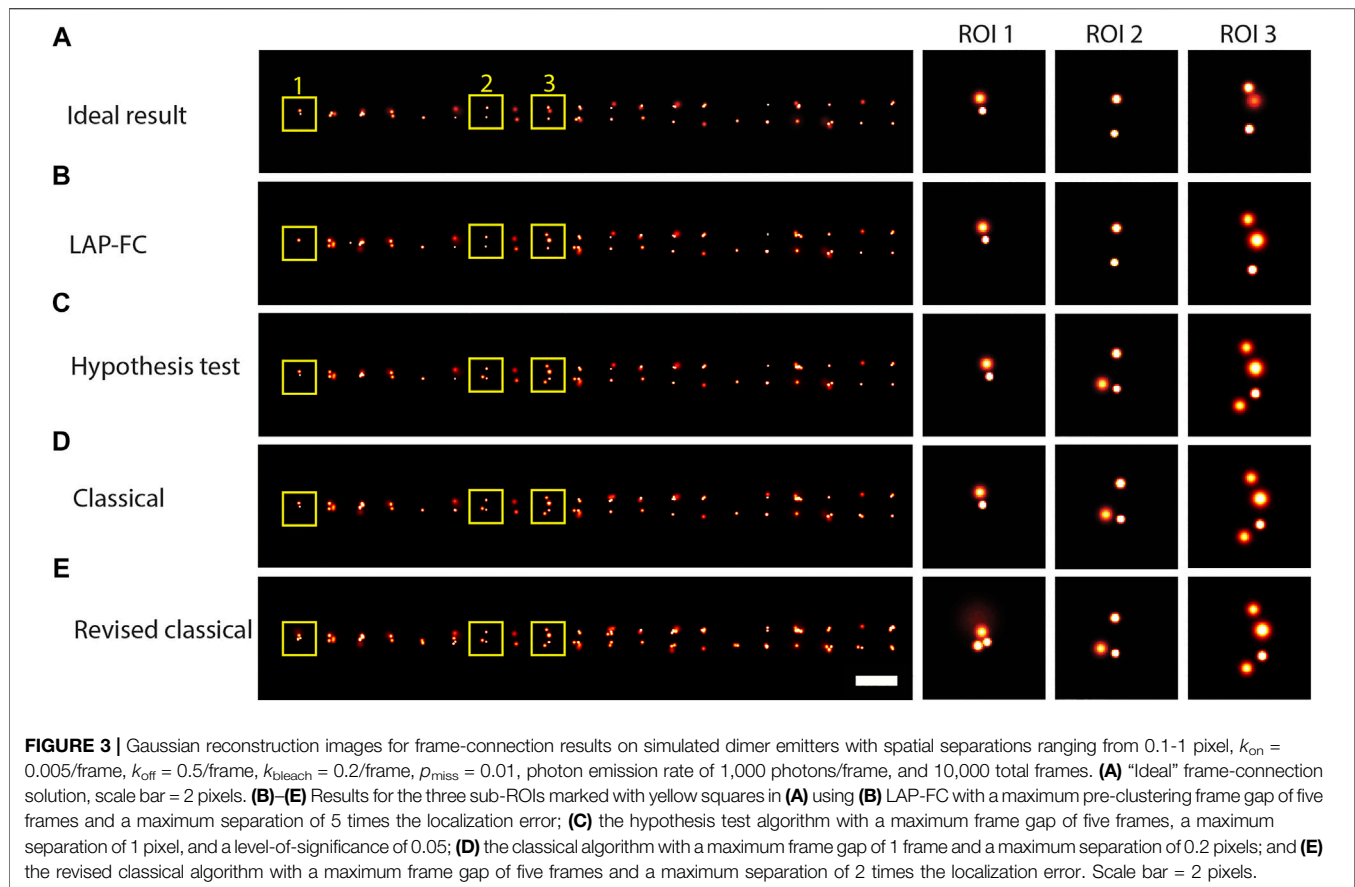


$$\hat{\sigma}^2 = \frac{1}{\sum_{i=1}^m 1/\sigma_i^2} \quad (5)$$

2.4 Simulated SMLM Data

Simulated SMLM localizations were generated to test the frame-connection algorithms. A uniformly distributed point target was simulated by scattering emitters uniformly across a square region of interest (ROI). Dimerized emitters were simulated by placing emitters at varying separations from one another with sufficient inter-dimer spacing to ensure localizations from distinct dimers

will not be connected by any of the algorithms. To generate localizations from simulated emitter positions, the frames in which each emitter was observed were simulated by the Gillespie algorithm (Gillespie, 1976) as prescribed by the transition rates $k_{\text{on}} = 0.005$ frame⁻¹, $k_{\text{off}} = 0.5$ frame⁻¹, and $k_{\text{bleach}} = 0.2$ frame⁻¹. Localizations corresponding to the emitter being on the entire frame were assigned a fixed photon count I . For frames in which the emitter turned on, turned off, or bleached, the number of photons was reduced to $I(1 - u)$ where u is sampled from the standard uniform distribution. Gaussian noise was added to each localization



with a standard deviation given by the Cramér-Rao lower bound corresponding to fitting a Gaussian to the emitter PSF given the background intensity and a finite pixel size (Smith et al., 2010). To mimic noise sources not accounted for by localization errors, such as residual, uncorrected sample drift, an additional source of Gaussian noise with standard deviation 0.05 pixels was added to each localization. A constant probability of missing a localization p_{miss} was applied to the final results by randomly removing $p_{\text{miss}}n$ (rounded to the nearest integer) localizations from the n total localizations.

2.5 Comparison to “Ideal” Results

The “ideal” frame-connection results are specified as follows. For a given simulation, the underlying emitter generating each localization is noted. Localizations arising from the same emitter that occur within five frames of one another are then combined using Eqs. 4, 5. These frame-connected localizations are considered to be the “ideal” frame-connection result.

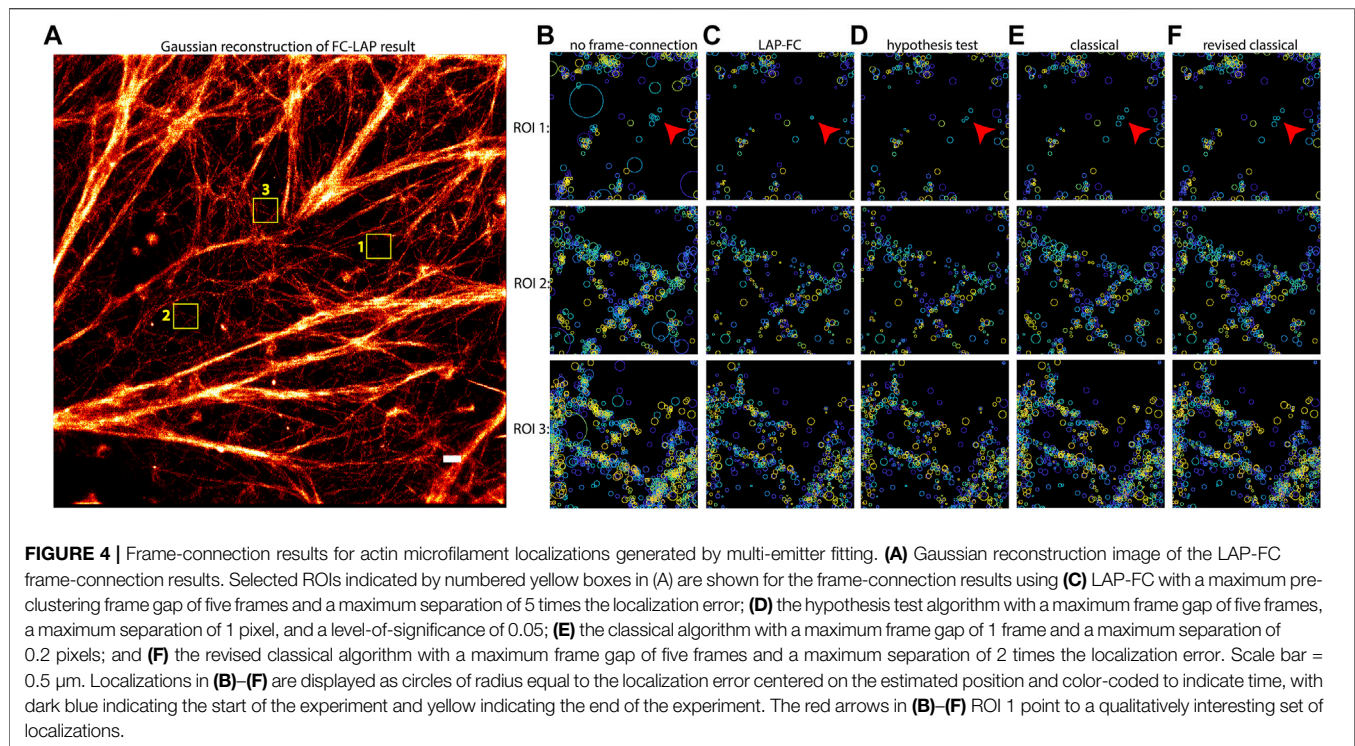
The cumulative distribution function (CDF) of the nearest-neighbor distance distribution between frame-connected localizations was computed as follows. For a given set of frame-connected localizations, the nearest-neighbor to each localization within five frames (in the past or into the future, but excluding same frame neighbors) was found and their separation was stored. The binned CDF was then computed from the resulting set of nearest-neighbor distances.

Comparisons to the “ideal” frame-connection CDF F_{ideal} were made by subtracting F_{ideal} from the binned CDF F of the results being compared. The difference $\delta \equiv F - F_{\text{ideal}}$ provides a visual tool for comparing frame-connection results. A deviation $\delta < 0$ suggests that localizations were connected that should not have been, since such over-connection would increase the expected nearest-neighbor distance. Similarly, a difference $\delta > 0$ suggests that frame-connection did not connect localizations which should have ideally been connected. Although this trend for δ may not necessarily hold for exceptionally high localization densities (e.g., for very high localization densities, incorrect connections may in fact cause the mean nearest-neighbor distance to decrease), we don’t expect such data to be relevant in SMLM.

3 RESULTS

3.1 Uniformly Distributed Emitters

Simulated SMLM data for uniformly distributed emitters was generated as described in section 2.4. The frame-connection results from each of the algorithms (LAP-FC, hypothesis test, classical, and revised classical) are shown in Figure 1. ROI selections were made to highlight the performance of LAP-FC in comparison to the other algorithms. For the sole emitter blink present in Figure 1 ROI 1, the LAP-FC algorithm was the only



method to completely connect all observed localizations. For **Figure 1** ROI 2, the hypothesis test, classical, and revised classical algorithms correctly connected most of the localizations. For **Figure 1** ROI 3, the classical and revised classical algorithms again connected most localizations correctly while failing to connect some others.

To compare the frame-connection algorithms for data with varying densities, a total of 40, 20, and 10 independent uniform emitter simulations were generated for initial emitter densities of $\rho_0 = 5$ emitters/pixel², $\rho_0 = 10$ emitters/pixel², and $\rho_0 = 20$ emitters/pixel², respectively, with the parameters otherwise matching those described in **section 2.4**. The deviation δ of the nearest-neighbor distance CDF from the ideal CDF was computed as described in **section 2.5**. The results are shown in **Figure 2**. For a relatively low initial emitter density of 5 emitters/pixel², all of the algorithms tend to under-cluster localizations, with LAP-FC showing closer correspondence to the ideal case; however, the hypothesis-test may slightly over-cluster as indicated by the dip of $\delta < 0$ in **Figure 2A**. For an initial density of 10 emitters/pixel², the hypothesis test algorithm shows the closest correspondence to the ideal frame-connection results, however the dip $\delta < 0$ seen in **Figure 2B** suggestive of over-clustering is more prominent than in **Figure 2A**. The LAP-FC algorithm shows the closest correspondence to the ideal result without indication of over-clustering. For an initial emitter density of 20 emitters/pixel², **Figure 2C** suggests that the hypothesis testing method is largely over-clustering localizations. The LAP-FC algorithm otherwise shows the closest correspondence to the ideal frame-connection results without significant over-clustering, however a small dip of $\delta < 0$ was present at a scale not visible in the figure.

For the simulations described in the preceding paragraph, histograms of the durations of frame-connected localizations were generated and are shown in **Supplementary Figure S2**. Comparing to the expected distribution (geometric with probability $p = 1 - \exp(-k)$, where $k \equiv k_{\text{off}} + k_{\text{bleach}}$) of frame-connected durations, all methods appear to have an over-abundance of short durations, with the trend being similar at each tested density. LAP-FC and the hypothesis test method more closely reproduce the expected distribution than the classical and revised classical methods, with the hypothesis test showing the closest correspondence.

To test the robustness of LAP-FC with respect to its estimates of k_{on} , k_{off} , k_{bleach} , and p_{miss} , LAP-FC was repeated for the 20 $\rho_0 = 10$ emitters/pixel² simulations described above with varying values of each parameter. For each of the 20 simulations, LAP-FC was applied and the internally estimated values \hat{k}_{on} , \hat{k}_{off} , \hat{k}_{bleach} , and \hat{p}_{miss} were noted (see **Supplementary Table S1**). LAP-FC was then applied to each simulation with externally prescribed values of k_{on} , k_{off} , k_{bleach} , and p_{miss} , with each parameter being varied individually with the other parameters held fixed at their true simulated value. Each parameter was varied to their upper and lower bound (see **Supplementary Text 1**) as well as to the maximum and minimum values estimated in the original LAP-FC application described above. The resulting values of δ were computed as described in 2.5 and plotted in **Supplementary Figure S1**. According to the results in **Supplementary Figure S1**, even large deviations in parameter estimates from the true values rarely lead to over-clustering by LAP-FC, and in all observed cases (i.e., excluding the upper and lower bound demonstrations), the results show little deviation from those when all parameters are set to their simulated value.

3.2 Simulated Dimer Emitters

Dimerized emitters were simulated at 20 spatial separations ranging uniformly from 0.1-1 pixel to investigate frame-connection performance for closely spaced emitters. Gaussian reconstruction images are shown for the results of each of the frame-connection algorithms in **Figure 3**. Overall, each of the tested algorithms performed well enough to observe the general trend in the data clear from the ideal result in **Figure 3A** (that is, pairs of closely spaced emitters with an increasing pair separation from left to right). The classical and the revised classical methods (**Figure 3D,E**, respectively) did not correctly connect as many localizations as the LAP-FC and hypothesis test methods (**Figure 3B,C**, respectively), however no over-clustering was apparent. Overall, the LAP-FC performed better than the other methods tested. No apparent over-clustering artifacts were introduced by any of the four algorithms tested.

3.3 High Duty Cycle Actin With Multi-Emitter Fitting

An SMLM dataset resulting from Bayesian multi-emitter fitting (Fazel et al., 2019a) of actin data with a relatively high localization density was used to compare the performance of the tested frame-connection algorithms. The results are shown in **Figure 4**. Inspecting the ROI selections made in **Figures 4C–F** and comparing to the non-frame connected results in **Figure 4B**, each of the algorithms appear to make reasonable connections based on localization spatiotemporal proximity. The LAP-FC and hypothesis testing algorithms made the most connections as is noticeable by the feature sharpness in **Figures 4C,D**. The classical and revised classical methods both fail to connect a pair of relatively isolated nearby emitters on the right hand side of ROI 1 (shown as blue circles and pointed to by small red arrows), which when compared to **Figure 4B** seem to be arising from the same emitter.

4 DISCUSSION

SMLM is rapidly becoming a commonplace tool for researchers in need of nanoscale spatial resolution in fluorescence microscopy. The expansion of SMLM outside of dedicated research labs necessitates reliable analyses which can be trusted without expert intervention. Quantitative analysis of the resulting super-resolved localizations requires, in many cases, a well-characterized correspondence between localizations and emitters. That is to say, many analyses of super-resolved localizations require a one-to-one relationship between localization and emitter. While recent techniques have largely solved this localization clustering problem (Fazel et al., 2019b), any such method will be limited by the reliability of the input localizations. If the input localizations contain a very large proportion of repeated localizations, such post-processing tools may be pushed to their practical limits, for example leading to infeasible computational costs. Alternatively, localizations which have been over-clustered (i.e., localizations from distinct emitters that were connected together) represent a loss of information unlikely to be captured by any post-processing analysis.

Many steps in SMLM data analysis have been refined and validated (e.g., fitting the localizations and determining the error in their positions), however the frame-connection problem has received little attention. Known existing methods for solving the frame-connection problem have not reached an optimal solution. We have shown that the classical and the revised classical methods are perhaps too conservative in their assignment of connections to make optimal use of the data. On the other hand, the hypothesis testing method is perhaps too liberal in its assignment of connections. We have shown that the hypothesis testing method for frame-connection, which typically provides more appealing results than the classical and revised classical methods, is susceptible to over-clustering at high densities. Furthermore, results of the classical, revised classical, and the hypothesis test algorithms rely heavily on the selection of arbitrary thresholds. We have shown that, by formulating the frame-connection problem as a linear assignment problem with statistically motivated assignment costs, these common artifacts can largely be reduced, with the added benefit that arbitrary thresholds are used only in a pre-processing step. Our algorithm accounts for the local emitter densities, the kinetic rates of blinking, and the possibility of missing localizations of a visible emitter. By combining all of this knowledge, our algorithm exceeds the performance of other known frame-connection problems with minimal to no over-clustering.

DATA AVAILABILITY STATEMENT

The raw data supporting the conclusions of this article will be made available by the authors, without undue reservation.

AUTHOR CONTRIBUTIONS

DS and KL were jointly involved in all aspects of the paper including conception of the algorithm and preparation of the article.

FUNDING

DS and KL were supported by NIH grants R21GM132716 and R01CA248166. KL was additionally supported by NIH grant P30CA118100.

ACKNOWLEDGMENTS

We thank Dr. Michael J. Wester for providing feedback during article preparation. We would also like to thank Dr. Hanieh Mazloom-Farsibaf for the actin dataset and Dr. Mohamadreza Fazel for Bayesian multi-emitter fitting analysis of the actin dataset.

SUPPLEMENTARY MATERIAL

The Supplementary Material for this article can be found online at: <https://www.frontiersin.org/articles/10.3389/fbinf.2021.724325/full#supplementary-material>

REFERENCES

- Betzig, E., Patterson, G. H., Sougrat, R., Lindwasser, O. W., Olenych, S., Bonifacino, J. S., et al. (2006). Imaging Intracellular Fluorescent Proteins at Nanometer Resolution. *Science* 313, 1642–1645. doi:10.1126/science.1127344
- Daszykowski, M., Walczak, B., and Massart, D. L. (2001). Looking for Natural Patterns in Data. *Chemometrics Intell. Lab. Syst.* 56, 83–92. doi:10.1016/S0169-7439(01)00111-3
- Deschout, H., Cella Zanacchi, F., Mlodzianoski, M., Diaspro, A., Bewersdorf, J., Hess, S. T., et al. (2014). Precisely and Accurately Localizing Single Emitters in Fluorescence Microscopy. *Nat. Methods* 11, 253–266. doi:10.1038/nmeth.2843
- Fazel, M., Wester, M. J., Mazloom-Farsibaf, H., Meddens, M. B. M., Eklund, A. S., Schlichthaerle, T., et al. (2019a). Bayesian Multiple Emitter Fitting Using Reversible Jump Markov Chain Monte Carlo. *Sci. Rep.* 9, 13791. doi:10.1038/s41598-019-50232-x
- Fazel, M., Wester, M. J., Rieger, B., Jungmann, R., and Lidke, K. A. (2019b). Sub-Nanometer Precision Using Bayesian Grouping of Localizations. *bioRxiv*, 752287. doi:10.1101/752287
- Gillespie, D. T. (1976). A General Method for Numerically Simulating the Stochastic Time Evolution of Coupled Chemical Reactions. *J. Comput. Phys.* 22, 403–434. doi:10.1016/0021-9991(76)90041-3
- Heilemann, M., Van De Linde, S., Schüttelpelz, M., Kasper, R., Seefeldt, B., Mukherjee, A., et al. (2008). Subdiffraction-resolution Fluorescence Imaging with Conventional Fluorescent Probes. *Angew. Chem. Int. Ed. Engl.* 47, 6172–6176. doi:10.1002/anie.200802376
- Hess, S. T., Girirajan, T. P., and Mason, M. D. (2006). Ultra-high Resolution Imaging by Fluorescence Photoactivation Localization Microscopy. *Biophys. J.* 91, 4258–4272. doi:10.1529/biophysj.106.091116
- Jaqaman, K., Loerke, D., Mettlen, M., Kuwata, H., Grinstein, S., Schmid, S. L., et al. (2008). Robust Single-Particle Tracking in Live-Cell Time-Lapse Sequences. *Nat. Methods* 5, 695–702. doi:10.1038/nmeth.1237
- Jonker, R., and Volgenant, A. (1987). A Shortest Augmenting Path Algorithm for Dense and Sparse Linear Assignment Problems. *Computing* 38, 325–340. doi:10.1007/bf02278710
- Jungmann, R., Steinhauer, C., Scheible, M., Kuzyk, A., Tinnefeld, P., and Simmel, F. C. (2010). Single-molecule Kinetics and Super-resolution Microscopy by Fluorescence Imaging of Transient Binding on DNA Origami. *Nano Lett.* 10, 4756–4761. doi:10.1021/nl103427w
- Levet, F., Hossy, E., Kechkar, A., Butler, C., Beghin, A., Choquet, D., et al. (2015). SR-tesseler: a Method to Segment and Quantify Localization-Based Super-resolution Microscopy Data. *Nat. Methods* 12, 1065–1071. doi:10.1038/nmeth.3579
- Marin, Z., Graff, M., Barentine, A. E. S., Soeller, C., Chung, K. K. H., Fuentes, L. A., et al. (2021). PYMEVisualize: an Open-Source Tool for Exploring 3D Super-resolution Data. *Nat. Methods* 18, 582–584. doi:10.1038/s41592-021-01165-9
- Nino, D. F., and Milstein, J. N. (2021). Estimating the Dynamic Range of Quantitative Single-Molecule Localization Microscopy. *bioRxiv*. doi:10.1101/2021.05.24.445502
- Ovesný, M., Křížek, P., Borkovec, J., Švindrych, Z., and Hagen, G. M. (2014). ThunderSTORM: A Comprehensive ImageJ Plug-In for PALM and STORM Data Analysis and Super-resolution Imaging. *Bioinformatics* 30, 2389–2390. doi:10.1093/bioinformatics/btu202
- Rust, M. J., Bates, M., and Zhuang, X. (2006). Sub-diffraction-limit Imaging by Stochastic Optical Reconstruction Microscopy (STORM). *Nat. Methods* 3, 793–795. doi:10.1038/nmeth929
- Sage, D., Pham, T. A., Babcock, H., Lukes, T., Pengo, T., Chao, J., et al. (2019). Super-resolution Fight Club: Assessment of 2D and 3D Single-Molecule Localization Microscopy Software. *Nat. Methods* 16, 387–395. doi:10.1038/s41592-019-0364-4
- Sergé, A., Bertaux, N., Rigneault, H., and Marguet, D. (2008). Dynamic Multiple-Target Tracing to Probe Spatiotemporal Cartography of Cell Membranes. *Nat. Methods* 5, 687–694. doi:10.1038/nmeth.1233
- Small, A., and Stahlheber, S. (2014). Fluorophore Localization Algorithms for Super-resolution Microscopy. *Nat. Methods* 11, 267–279. doi:10.1038/nmeth.2844
- Smith, C. S., Joseph, N., Rieger, B., and Lidke, K. A. (2010). Fast, Single-Molecule Localization that Achieves Theoretically Minimum Uncertainty. *Nat. Methods* 7, 373–375. doi:10.1038/nmeth.1449
- Wester, M. J., Schodt, D. J., Mazloom-Farsibaf, H., Fazel, M., Pallikkuth, S., and Lidke, K. A. (2021). Robust, Fiducial-free Drift Correction for Super-resolution Imaging. *bioRxiv*. doi:10.1101/2021.03.26.437196

Conflict of Interest: The authors declare that the research was conducted in the absence of any commercial or financial relationships that could be construed as a potential conflict of interest.

Publisher's Note: All claims expressed in this article are solely those of the authors and do not necessarily represent those of their affiliated organizations, or those of the publisher, the editors and the reviewers. Any product that may be evaluated in this article, or claim that may be made by its manufacturer, is not guaranteed or endorsed by the publisher.

Copyright © 2021 Schodt and Lidke. This is an open-access article distributed under the terms of the Creative Commons Attribution License (CC BY). The use, distribution or reproduction in other forums is permitted, provided the original author(s) and the copyright owner(s) are credited and that the original publication in this journal is cited, in accordance with accepted academic practice. No use, distribution or reproduction is permitted which does not comply with these terms.